



**Molecular structure of (4(4-cyanobenzoyl) phenyl)  
1,5-dithio-beta-D-xylopyranoside (naroparcil) in the  
solid state and in solution: an investigation by X-ray  
crystallography, molecular mechanics calculations, and  
NMR spectroscopy**

J.Y. Le Questel, N. Mouhous-Riou, Sarah Perez

► **To cite this version:**

J.Y. Le Questel, N. Mouhous-Riou, Sarah Perez. Molecular structure of (4(4-cyanobenzoyl) phenyl) 1,5-dithio-beta-D-xylopyranoside (naroparcil) in the solid state and in solution: an investigation by X-ray crystallography, molecular mechanics calculations, and NMR spectroscopy. Carbohydrate Research, 1996, 284, pp.35-49. hal-02694819

**HAL Id: hal-02694819**

**<https://hal.inrae.fr/hal-02694819v1>**

Submitted on 1 Jun 2020

**HAL** is a multi-disciplinary open access archive for the deposit and dissemination of scientific research documents, whether they are published or not. The documents may come from teaching and research institutions in France or abroad, or from public or private research centers.

L'archive ouverte pluridisciplinaire **HAL**, est destinée au dépôt et à la diffusion de documents scientifiques de niveau recherche, publiés ou non, émanant des établissements d'enseignement et de recherche français ou étrangers, des laboratoires publics ou privés.

# Molecular structure of [4-(4-cyanobenzoyl) phenyl] 1,5-dithio- $\beta$ -D-xylopyranoside (naroparcil) in the solid state and in solution: an investigation by X-ray crystallography, molecular mechanics calculations, and NMR spectroscopy<sup>1</sup>

Jean-Yves Le Questel<sup>2</sup>, Nadine Mouhous-Riou, Serge Pérez<sup>\*</sup>

*Ingénierie Moléculaire, Institut National de la Recherche Agronomique, BP1627, 44316 Nantes Cédex 03, France*

Received 26 October 1995; accepted 8 January 1996

## Abstract

The conformational behavior of a representative of a new class of oral venous antithrombotic agents, [4-(4-cyanobenzoyl) phenyl] 1,5-dithio- $\beta$ -D-xylopyranoside (naroparcil) (**1**) has been characterized by X-ray crystallography, molecular modeling and NMR studies. The crystal structure of **1** belongs to the monoclinic space group  $P2_1$ , with two independent molecules in the asymmetric unit. The unit cell has dimensions of  $a = 11.641$ ,  $b = 8.040$ ,  $c = 20.020$  Å, and  $\beta = 102.29^\circ$ . The present work provides structural information on the influence of substitution of intracyclic and glycosidic oxygen atoms by sulfur atoms, as well as on the influence of aromatic rings on the carbohydrate moiety. The xylopyranoside ring has the classical  ${}^4C_1$  conformation. As for the orientations of the phenyl substituent with respect to the xylopyranose the values observed in the two independent molecules are strikingly different ( $-85^\circ$ ,  $-177^\circ$ ) and ( $-102^\circ$ ,  $144^\circ$ ). The  ${}^1\text{H}$ – ${}^1\text{H}$  NOE across the glycosidic bond has been measured by NOESY experiments. In parallel, a conformational analysis using the crystal coordinates as the starting point has been made using the Tripos force field. The resulting potential energy surface indicates a high flexibility about the glycosidic linkage. The theoretical NMR data were calculated taking into account all the

<sup>\*</sup> Corresponding author. Present address: Centre de Recherches sur les Macromolécules Végétales, CNRS, BP 53X, 38041 Grenoble, France. Tel.: (33)-40-67-50-43; fax: (33)-40-67-50-92; e-mail: perez@nantes.inra.fr

<sup>1</sup> Data deposited with CSD.

<sup>2</sup> Present address: Laboratoire de Spectrochimie Moléculaire, Faculté des Sciences et Techniques, Université de Nantes, Nantes, France.

accessible conformations and using the averaging methods appropriate for slow internal motions. The agreement between experimental and theoretical data is excellent and constitutes a satisfactory test of the validity of the conformational energy surface.

**Keywords:** Thio-sugars; Glycosaminoglycan; X-ray crystallography; High resolution NMR spectroscopy; Molecular mechanics

## 1. Introduction

The synthesis of glycosaminoglycan may be induced by exogeneous primers such as  $\beta$ -D-xylopyranosyl derivatives. Although the biological process associated with such a synthesis is not completely deciphered, there is interest in elucidating the three-dimensional features that characterize these inducers. Actually some of them displaying antithrombotic activity have been already evaluated in different animal models [1]. The doses required for biological activity are however high. In order to design compounds active at lower doses, the heteroatom of these derivatives has been changed, and thioanalogs have in particular been synthesized [2]. In terms of structure activity relationships, the 5-thioxylopyranoside derivatives are more potent as oral venous antithrombotic agents than the corresponding xylopyranosides. Replacement of the oxygen atom of the thioxyloside bond by sulfur gives the 1,5-dithioxylosides, these compounds being equipotent than the 1-oxygenated analogs [2].

In order to relate the structural features of such molecules to their physical and biological properties, a detailed description of their conformational preferences is required. The crystal structures of a few members of this family have recently been reported [3,4]. In the present work, the elucidation of the molecular and crystalline structure of [4-(4-cyanobenzoyl) phenyl] 1,5-dithio- $\beta$ -D-xylopyranoside (naroparcil) (**1**) has been undertaken through the combined use of X-ray diffraction, molecular mechanics calculations and NMR spectroscopy.

## 2. Experimental

**Nomenclature.**—The recommendation and symbols proposed by the Joint Commission on Biochemical Nomenclature [5] are used throughout this paper. A schematic representation of **1**, along with the labeling of the atoms, is given in Fig. 1. The relative orientation of a pair of contiguous residues is described by the torsion angles  $\Phi$ ,  $\Psi$ , and  $\Phi_H$ ,  $\Psi_H$  respectively defined as:

$$\Phi = \text{S-5-C-1-S-1-C-6} \quad \Phi_H = \text{H-1-C-1-S-1-C-6}$$

$$\Psi = \text{C-1-S-1-C-6-C-7} \quad \Psi_H = \text{C-1-S-1-C-6-H-6}$$

**Crystal structure resolution.**—Crystals of **1** were grown by slow evaporation from a methanolic solution at room temperature. A single crystal of dimension  $0.01 \times 0.15 \times 0.50$  mm was used. Accurate unit-cell parameters were determined by a least-squares fit to the setting angles at high  $2\theta$  values. Lorentz and polarization corrections were

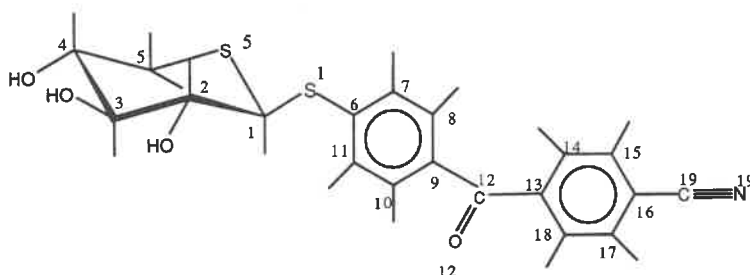


Fig. 1. Schematic representation of [4-(4-cyanobenzoyl) phenyl] 1,5-dithio- $\beta$ -D-xylopyranoside together with the labeling of some atoms.

applied. No absorption correction has been made since the crystal dimensions are small. The unit-cell parameters and crystallographic data of interest are given in Table 1.

The intensities of 3510 independent reflections were measured inside the sphere limited by  $2\theta < 125^\circ$  at the Cu wavelength using the “flying step-scanning” mode on a Philips PW1100 diffractometer. The average of three reference reflections monitored each hour showed no noticeable decrease during the data collection time. All the intensities were corrected from the background noise. From the 3510 measured reflections, 2805 with  $I/\sigma(I) > 2\sigma$  were considered as observed. Scattering factors were taken from the International Tables of Crystallography [6]. The structure was solved by direct methods [7,8] allowing the location of all C, O, S, and N atoms. The H atoms were located by successive difference Fourier maps and isotropic refinement. The last refinement cycles were performed using anisotropic thermal temperature factors for the non-hydrogen atoms, whereas the hydrogen atoms were assigned an isotropic temperature factor. During the refinement, each reflection was given a weight  $w = 1/\sigma(F_o)^2$  derived from  $\sigma(I)$ . The final  $R$  value was 0.048 and  $R_w = 0.0508$ . A final electron density map showed no significant residual density.

Table 1

Crystal data and structure determination data for [4-(4-cyanobenzoyl) phenyl] 1,5-dithio- $\beta$ -D-xylopyranoside

Molecular formula	$C_{19}H_{17}NO_4S_2, H_2O$
Molar mass	387.48 + 18
Crystal system	Monoclinic
Space group	$P2_1$
Z	4
$a$ (Å)	11.641(4)
$b$ (Å)	8.040(3)
$c$ (Å)	20.020(3)
$\beta$	102.29(3)
$D_c$ (kg dm $^{-3}$ )	1.40
Crystal size (mm)	$0.01 \times 0.15 \times 0.50$
$F(000)$ (e $^{-}$ )	808
$T$ (K)	290

**NMR spectroscopy.**— $^1\text{H}$  (400.13 MHz) spectra were recorded in  $\text{Me}_2\text{SO}-d_6$  with a Bruker instrument operating in the Fourier-transform mode at 296 K. The  $^1\text{H}$  chemical shifts of **1** have been assigned from homo-nuclear correlation spectroscopy. The  $^3J_{\text{H-H}}$  were extracted from a spectrum with a digital resolution of 0.12 Hz/pt. The  $^1\text{H}$   $T_1$  measurements were acquired with the inversion-recovery sequence ( $180 - t - 90 - \text{FID}$ ) and relaxation times were calculated with the Bruker  $T_1$  routine. In the case of selective  $^1\text{H}$  relaxation times, the duration of the soft  $180^\circ$  pulse, which was performed with the Dante sequence, was 20 ms. Phase-sensitive NOESY [9] were acquired with mixing times of 0 and 1 s. A 20 ms variable delay was introduced at the beginning of the mixing time in order to suppress  $J$ -peak transfer. The recycle time was set to five times the longest  $T_1$  to ensure that the normalized NOESY volume matrix would be symmetrical. A total of  $512\text{K} \times 1\text{K}$  data matrices were obtained and zero-filled to  $1\text{K} \times 1\text{K}$ . Prior to Fourier transformation the first data file was halved to reduce  $t_1$  ridges, and  $\pi/2$ -shifted sine-squared weighting functions were applied [10]. It is worth noticing that the NOE effect decreases with the correlation time itself affected by parameters such as solvent viscosity and the radius of the molecule. In the present study, both parameters have contributed to increase the  $\tau_c$ , which is estimated at  $1.5 \times 10^{-10}$  s for **1**. These conditions have made the evaluation of the NOESY cross-peak intensities a delicate operation. They were evaluated from the summed  $\omega_1$  subspectra contributing to a specific signal. The values of the normalized  $a_{ij}$  and  $a_{ji}$  elements were averaged before back-transformation to the relaxation matrix [11] with in house software.

**Molecular mechanics calculations.**—*Energy calculations and geometry optimization.* The Tripos force field [12] is a classic molecular mechanics method in which the potential energy is evaluated as a combination of several potential energy functions [13]. All the energy parameters are stored in tables which can be modified or extended. The Tripos force field has been the subject of a recent parameterization and a molecular mechanical force field capable of performing conformational analysis of oligosaccharides has been derived [14]. For the present work, a set of new parameters characteristic of a substitution of the intracyclic (or) and glycosidic oxygen atoms by sulfur atoms has been added to the 6.0 version of the force field making it suitable for the molecular modeling of thioanalogs of carbohydrates [15]. The MAXIMIN2 procedure of the SYBYL molecular modeling package, which consists of an energy minimizer using a combination of first and non-derivatives methods has been used [16].

**Rigid-residue conformational analysis.** The SEARCH procedure of SYBYL allows for a systematic conformational search. In this procedure a set of rotatable bonds is identified and, for each conformation achieved by this set of rotations, all internal distances are computed. A conformation is rejected if any of the distances is less than the sum of the van der Waals radii of the interacting atoms. The van der Waals radii sum can be altered by an overall multiplication constant which can “soften” the criterion. For acceptable conformations the potential energy can be calculated using the Tripos force field. The allowed conformations and their energies were determined using the Tripos force field and the SEARCH procedure. The starting geometry was taken from the crystal structure of **1**; **1B** was selected because it follows the trends observed in aryl pyranosides structures (vide infra). The potential energy surface was then computed for **1** and the glycosidic torsional angles  $\Phi$ ,  $\Psi$  examined over the whole angular range. The

computations were performed with the rigid residue approximation using the appropriate atom types and the parameters for the oxygen–sulfur atoms substitution. The  $\Phi$  and  $\Psi$  torsional angles were incremented by steps of  $5^\circ$  during the SEARCH option of SYBYL. With respect to the energy minimum the iso-energy contours were drawn by interpolation at  $1 \text{ kcal mol}^{-1}$  intervals and the  $10 \text{ kcal mol}^{-1}$  contour was selected as the outer limit.

*Calculations of theoretical NMR parameters.*—Averaging is required to correctly predict properties of a population of conformations. Using the Boltzmann distribution, the relative population of each conformer is given by the expression:

$$P_i = \exp(-E_i/kT) / \sum \exp(-E_i/kT)$$

For a NMR parameter  $S$  depending in a non-linear way on an associated structural parameter  $S_i$ , the average value can be computed by

$$\langle M \rangle = \sum P_i f(S_i)$$

Equations for the calculation of the several  $\langle {}^3J_{\text{H-H}} \rangle$  of the ring were established according to a known method. For the NOESY conditions, the ensemble average cross-relaxation matrix  $\langle R \rangle$  was calculated from the  $\langle r^{-6} \rangle$  values following previously published procedures [11]. The spectral density functions used in these calculations are appropriate for a molecule undergoing isotropic tumbling. It is also assumed that the internal motion is slow compared to the overall motion.

### 3. Results and discussion

*Molecular conformation in the solid state.*—A representation of the pair of symmetry independent molecules **1A** and **1B**, together with the water molecule forming the asymmetric content of a crystal of **1** is shown in Fig. 2. The representations which depict the anisotropic temperature factors have been obtained with the aid of the PLUTON program [17]. The positional and isotropic thermal parameters for the non-hydrogen atoms are given in Table 2. Bond lengths and angles are reported in Table 3. The mean C–H distances for A and B are, respectively,  $0.99 \text{ \AA}$  (range  $0.86\text{--}1.12 \text{ \AA}$ ), and  $1.04 \text{ \AA}$  (range  $0.95\text{--}1.10 \text{ \AA}$ ), whereas the mean O–H distances are  $1.07 \text{ \AA}$  (range  $0.98\text{--}1.14 \text{ \AA}$ ) and  $0.96 \text{ \AA}$  (range  $0.98\text{--}1.01 \text{ \AA}$ ). The mean C–C distance in the phenyl groups is for both structures  $1.39 \text{ \AA}$ .

The crystal structural investigations of carbohydrates thioanalogs reported in the literature deal mainly with monosubstituted derivatives (either in the ring or in the glycosidic position [18–20]). To our knowledge, only one X-ray investigation has been reported for molecules substituted in both positions [21]. The present work therefore extends the structural data available on this family of compounds and can be used to analyze the structural influence of the oxygen–sulfur atom substitutions in both positions.

The geometrical characteristics of the xylopyranose rings of the two independent molecules are in agreement with the one reported for carbohydrate structures in which both intracyclic and glycosidic oxygen atoms have been substituted by a sulfur atom

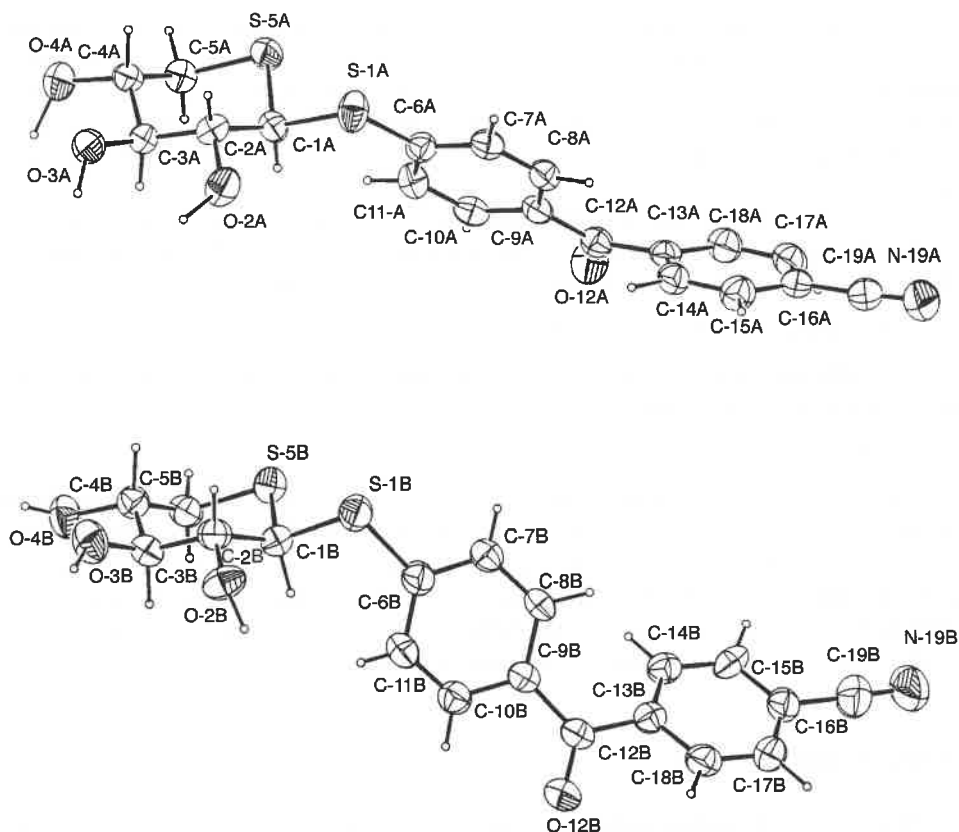


Fig. 2. ORTEP plot of [4-(4-cyanobenzoyl) phenyl] 1,5-dithio- $\beta$ -D-xylopyranoside in the crystal. Thermal ellipsoids at 50% probability.

[21]. The two xylopyranose residues have the expected  ${}^4C_1$  conformation. The internal C–C–C pyranose ring angles exhibit a significant opening: A, range 109.3–112.5°, mean 111.2°; B, range 112.1–112.7°, mean 112.3°. The endocyclic C–C–S angles have for both molecules an average of 111.8°. The exocyclic C–C–O bond angles show a wide variation: from 107.8° to 112.1°, with an average of 109.6° for A; from 106.7° to 110.1°, with an average of 108.5° for B. The endocyclic C1–S–S–C5 angle, of 97.4 and 99.9°, respectively, for A and B, is more acute than for a cyclic oxygen, this value being in agreement with the ones already reported for 1,5-dithiopyranosides [21]. The torsion angles around the pyranose rings and the glycosidic linkages are given in Table 4. As observed by Girling and Jeffrey [21], the angles about the C–S ring bonds are among the smallest torsion angles in the ring, whereas in the pyranose sugars, the corresponding C–O torsion angles are the largest.

The glycosidic linkage represents a molecular segment where two electronegative atoms bearing lone pairs of electrons are linked to the anomeric C atom. The electronic structure of this arrangement affects the geometry and conformation of the molecule, the

resulting consequences being termed the anomeric and exo-anomeric effect [22]. If their influence on molecular geometry is well described for the C–O–C–O–C sequence, this is not the case when oxygen(s) atom(s) is(are) substituted by sulfur(s) atom(s). This work illustrates the geometry of the C–S–C–S–C sequence. The bond-length distribution in the C-5–S-5–C-1–S-1 sequence does not follow the predicted and observed bond trends in methyl-pyranosides [23]. The mean value of the C-1–S-1 bond distances is 1.815 Å, being of the same order of magnitude than the standard value of 1.817 Å for a single C–S bond. For both molecules, the C-1–S-1 bonds are larger (**1A**: 1.826 Å, **1B**: 1.804 Å) than the S-1–C-6 distances (**1A**: 1.754 Å, **1B**: 1.766 Å). For one of the two independent molecules (**1B**), the C-5–S-5 bond is significantly shorter [1.789 (6) Å] than the S-5–C-1 distance [1.836 (5) Å]. Comparable differences in C–S bond lengths have been reported for 1,5-dithio- $\beta$ -D-pyranosides [21] and for 5-thio- $\beta$ -D-pyranosides [24]. For the molecule **1A**, however, the C-5–S-5 and S-5–C-1 distances of 1.814 and 1.815 Å, respectively, are close to the standard value of 1.817 Å.

The present results also illustrate how the geometry at the anomeric center is influenced by an aromatic ring. Such structural data are available for the C–O–C–O–C and C–S–C–O–C acetal fragments [25,3,4], but not for the C–S–C–S–C arrangement. The valence angles  $\tau$  C-1–S-1–C-6 (**1A**: 105.7° and **1B**: 104.9°) are larger than the mean value of 102.5° reported for 1,5-dithio- $\beta$ -D-pyranosides [21].

The orientation of the phenyl substituent with respect to the xylopyranose residue is described by the torsion angles  $\Phi$  (S-5–C-1–S-1–C-6) and  $\Psi$  (C-1–S-1–C-6–C-7). These angles have respective values of **1A**: –85°; **1B**: –102° and **1A**: –177°; **1B**: 144°. Only the torsion angles of the molecule **A** fall within the respective ranges of –65° to –85° and 180°  $\pm$  20° observed in aryl pyranoside structures [25]. In this case, the orientation of the aromatic ring is nearly coplanar with respect to the anomeric carbon atom C-1. This conformation favors the delocalization of the electrons from the lone-pair orbitals of the glycosidic S atoms to the  $p\pi$  orbitals of the phenyl ring. This may explain the significant opening of the  $\tau$  valence angle for **1A**. Another relevant geometric parameter of this molecule is the S-1–C-6 bond length of 1.754 (4) Å. This value is intermediate between those taken respectively by a S–C single (1.817 Å) and double bond (1.710 Å). Such a partial double-bond character could reflect the resonance of the glycosidic sulfur lone pairs with the aromatic ring. This behavior is not adopted by the molecule **1B** which shows a glycosidic valence angle greater (104.9°) than the mean value of 102.5° reported for 1,5-dithio- $\beta$ -D-pyranosides [21] but for which the glycosidic torsion angles do not follow the trends observed in aryl pyranosides.

Two orthogonal views of the packing of the molecules in the unit cell are displayed in Fig. 3. They help to illustrate the respective roles of hydrogen-bond and hydrophobic interactions in the three-dimensional arrangement. There are no intramolecular hydrogen bonds. The geometrical characteristics of intermolecular hydrogen bonds of **1** are given in Table 5. All secondary hydroxyl groups are involved in hydrogen bonding with neighboring secondary hydroxyl groups; each acts both as a donor and an acceptor except O-4–HO-4 and O-3–HO-3 of molecules **1A** and **1B**, respectively, which are only involved as donors. The water molecule uses all its hydrogen bonding capacities since it is tetrahedrally coordinated. The nitrogen atom of the nitrile group, which forms the end of the hydrophobic part of the molecule, utilizes its hydrogen bonding acceptor capacity.



Table 2

Atomic positional parameters and equivalent thermal parameters for [4-(4-cyanobenzoyl) phenyl] 1,5-dithio- $\beta$ -D-xylopyranoside

Atom	$x/a$	$y/b$	$z/c$	$U(\text{iso})$
S-1A	−0.20198 (9)	−0.03727 (2)	−0.77514 (5)	0.0474
S-5A	−0.3112 (1)	0.05350 (2)	−0.66235 (5)	0.0436
O-2A	−0.0845 (3)	−0.3127 (5)	−0.6817 (2)	0.0499
O-3A	−0.0566 (3)	−0.3111 (4)	−0.5411 (2)	0.0487
O-4A	−0.2200 (3)	−0.1622 (5)	−0.4773 (1)	0.0524
O-12A	−0.7093 (2)	−0.1425 (5)	−1.0057 (2)	0.0553
N-19A	−0.5788 (5)	−0.0353 (7)	−1.3520 (2)	0.0721
C-1A	−0.2429 (3)	−0.1181 (5)	−0.6982 (2)	0.0390
C-2A	−0.1333 (4)	−0.1829 (6)	−0.6489 (2)	0.0411
C-3A	−0.1620 (4)	−0.2456 (5)	−0.5822 (2)	0.0399
C-4A	−0.2089 (3)	−0.1090 (5)	−0.5430 (2)	0.0388
C-5A	−0.3272 (3)	−0.0494 (6)	−0.5842 (2)	0.0421
C-6A	−0.3281 (3)	−0.0565 (5)	−0.8406 (2)	0.0386
C-7A	−0.3129 (4)	−0.0089 (5)	−0.9047 (2)	0.0410
C-8A	−0.4027 (3)	−0.0261 (5)	−0.9616 (2)	0.0393
C-9A	−0.5118 (3)	−0.0915 (5)	−0.9557 (2)	0.0371
C-10A	−0.5272 (3)	−0.1355 (5)	−0.8911 (2)	0.0415
C-11A	−0.4376 (3)	−0.1190 (6)	−0.8338 (2)	0.0411
C-12A	−0.6112 (3)	−0.1125 (6)	−1.0151 (2)	0.0422
C-13A	−0.5954 (3)	−0.0953 (5)	−1.0869 (2)	0.0381
C-14A	−0.5014 (4)	−0.1619 (6)	−1.1109 (2)	0.0432
C-15A	−0.4980 (4)	−0.1522 (6)	−1.1788 (2)	0.0516
C-16A	−0.5885 (4)	−0.0748 (5)	−1.2251 (2)	0.0459
C-17A	−0.6850 (4)	−0.0116 (6)	−1.2022 (2)	0.0492
C-18A	−0.6863 (4)	−0.0215 (6)	−1.1342 (2)	0.0492
C-19A	−0.5833 (4)	−0.0563 (6)	−1.2954 (2)	0.0536
S-1B	−0.2689 (1)	0.0889 (2)	−0.25709 (6)	0.0543
S-5B	−0.38443 (9)	0.3929 (2)	−0.31158 (5)	0.0464
O-2B	−0.15661 (2)	0.0982 (5)	−0.3841 (2)	0.0541
O-3B	−0.2690 (3)	0.2678 (5)	−0.5043 (2)	0.0582
O-4B	−0.3756 (3)	0.5688 (5)	−0.4963 (2)	0.0564
O-12B	0.2014 (3)	0.2249 (6)	−0.0060 (2)	0.0605
O-31	−0.9234 (3)	−0.1420 (5)	−0.4391 (2)	0.0574
N-19B	0.0391 (5)	0.1930 (1)	0.3316 (2)	0.0879
C-1B	−0.2598 (4)	0.2581 (6)	−0.3149 (2)	0.0449
C-2B	−0.2599 (4)	0.1941 (6)	−0.3867 (2)	0.0451
C-3B	−0.2640 (4)	0.3362 (6)	−0.4382 (2)	0.0423
C-4B	−0.3722 (4)	0.4453 (6)	−0.4437 (2)	0.0435
C-5B	−0.3732 (4)	0.5367 (6)	−0.3781 (2)	0.0477
C-6B	−0.1620 (4)	0.1348 (6)	−0.1827 (2)	0.0436
C-7B	−0.1892 (4)	0.0930 (5)	−0.1200 (2)	0.0422
C-8B	−0.1059 (4)	0.1147 (5)	−0.0595 (2)	0.0405
C-9B	0.0039 (3)	0.1846 (6)	−0.0610 (2)	0.0398
C-10B	0.0276 (4)	0.2254 (6)	−0.1242 (2)	0.0434
C-11B	−0.0517 (4)	0.2010 (6)	−0.1836 (2)	0.0467
C-12B	0.1010 (4)	0.2018 (6)	0.0009 (2)	0.0422
C-13B	0.0790 (4)	0.1889 (5)	0.0709 (2)	0.0396
C-14B	−0.0202 (4)	0.2601 (6)	0.0896 (2)	0.0431

Table 2 (continued)

Atom	$x/a$	$y/b$	$z/c$	$U(\text{iso})$
C-15B	−0.0277 (4)	0.2622 (6)	0.1568 (2)	0.0477
C-16B	0.0617 (4)	0.1954 (6)	0.2063 (2)	0.0482
C-17B	0.1604 (4)	0.1257 (6)	0.1889 (2)	0.0508
C-18B	0.1687 (4)	0.1246 (6)	0.1219 (3)	0.0469
C-19B	0.0506 (5)	0.1943 (9)	0.2771 (3)	0.0645

The crystal packing is characterized by an alternation of hydrophilic and hydrophobic zones (Fig. 3). The neighboring molecules are first arranged so as to maximize their hydrophilic interactions through the network of hydrogen-bonds interactions. The hydrophilic, hydrogen bonded groups form a hydrophilic layer parallel to the crystallographic  $a$ ,  $b$  plane, and the aromatic rings are stacked to form a hydrophobic layer

Table 3

Bond lengths (Å) and angles (°) of **1A** and **1B**

Atom 1	Atom 2	Distance (Å)	
		<b>1A</b>	<b>1B</b>
C-1	C-2	1.529 (5)	1.526 (6)
C-2	C-3	1.528 (6)	1.533 (6)
C-3	C-4	1.517 (6)	1.519 (6)
C-4	C-5	1.524 (6)	1.509 (6)
C-1	S-1	1.826 (4)	1.804 (5)
C-1	S-5	1.815 (4)	1.824 (5)
C-2	O-2	1.415 (5)	1.420 (5)
C-3	O-3	1.425 (5)	1.421 (5)
C-4	O-4	1.415 (5)	1.442 (5)
C-5	S-5	1.814 (4)	1.789 (5)

Atom 1	Atom 2	Atom 3	Angle (°)	
			<b>1A</b>	<b>1B</b>
C-1	S-1	C-6	105.7 (2)	104.9 (2)
S-1	C-1	C-2	109.5 (3)	111.2 (3)
S-1	C-1	S-5	106.1 (2)	105.6 (2)
C-2	C-1	S-5	112.3 (3)	113.2 (3)
C-1	C-2	C-3	111.7 (3)	112.1 (4)
C-1	C-2	O-2	108.3 (3)	108.4 (3)
C-3	C-2	O-2	110.3 (4)	109.6 (4)
C-2	C-3	C-4	112.5 (4)	112.7 (3)
C-2	C-3	O-3	107.8 (3)	109.1 (4)
C-4	C-3	O-3	109.2 (3)	106.7 (4)
C-3	C-4	C-5	109.3 (3)	112.2 (4)
C-3	C-4	O-4	112.1 (4)	110.1 (3)
C-5	C-4	O-4	110.3 (3)	107.3 (4)
C-4	C-5	S-5	111.3 (3)	110.4 (3)
C-1	S-5	C-5	97.4 (2)	99.9 (2)

Table 4  
Torsion angles (°) of 1A and 1B

Atom 1	Atom 2	Atom 3	Atom 4	Angle (°)	
				1A	1B
S-5	C-1	S-1	C-6	−85.0	−102.4
C-1	S-1	C-6	C-7	−176.9	143.9
S-5	C-1	C-2	C-3	60.0	55.9
C-1	C-2	C-3	C-4	−62.5	−59.3
C-2	C-3	C-4	C-5	65.4	64.7
C-3	C-4	C-5	S-5	−66.5	−64.9
C-4	C-5	S-5	C-1	57.8	54.5
C-5	S-5	C-1	C-2	−54.2	−51.4
C-5	S-5	C-1	S-1	−173.9	−173.3
S-1	C-1	C-2	O-2	−60.8	−64.3
O-2	C-2	C-3	O-3	56.6	62.0
O-3	C-3	C-4	O-4	−52.3	−56.2

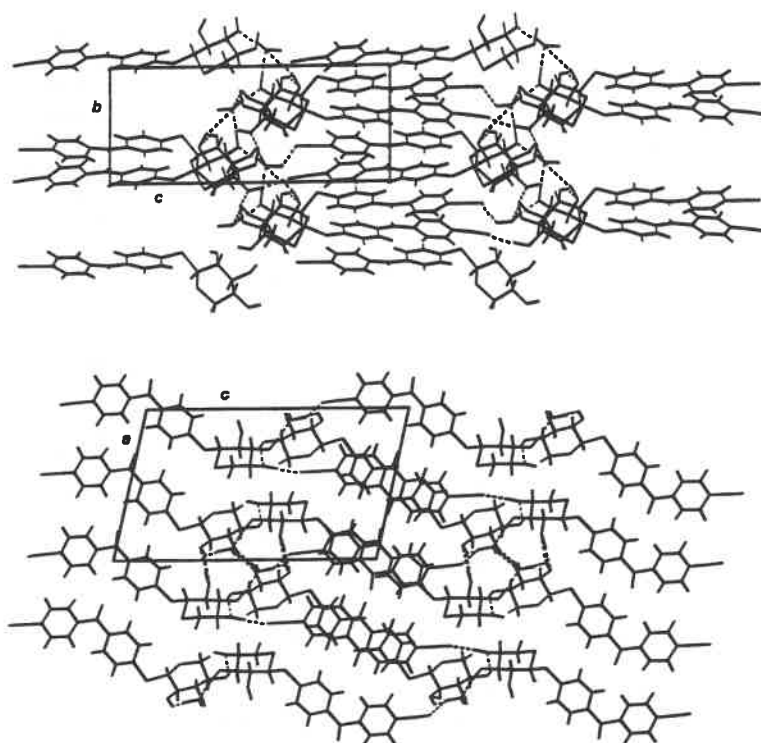


Fig. 3. Packing of the molecules of [4-(4-cyanobenzoyl) phenyl] 1,5-dithio- $\beta$ -D-xylopyranoside in the crystal. Hydrogen bonds are shown by dashed lines. (Top) View down the *a* axis; (bottom) view down the *b* axis.

Table 5

Hydrogen bonding in [4-(4-cyanobenzoyl) phenyl] 1,5-dithio- $\beta$ -D-xylopyranoside

Donor-H...acceptor <sup>a</sup>	D...A (Å)	D-H (Å)	H...A (Å)	D-H...A (°)
O-2A-HO-2A...O-2B II(-c)	2.08	1.08	2.184	123.4
O-3A-HO-3A...O-31 II(-a-c)	2.69	0.98	1.802	149.0
O-4A-HO-4A...O-4B I(b)	2.79	1.14	1.846	137.1
O-2B-HO-2B...O-2A II(-b-c)	2.92	0.98	2.021	152.4
O-3B-HO-3B...O-31 II(-a-b-c)	2.81	1.01	2.209	116.8
O-4B-HO-4B...N-19A II(-a-b+2c)	3.08	0.89	2.194	173.8
O-31-H-1-O-31...N-19B II(-a)	3.07	1.14	2.224	129.0
O-31-H-2-O-31...O-3A I(a)	2.66	0.84	1.821	171.8

<sup>a</sup> Equivalent positions: (I)  $x, y, z$ ; (II)  $-x, y+1/2, -z$ .

which is also parallel to the crystallographic  $a, b$  plane. As observed for the crystal structures of methyl 1-thio- $\alpha$ - [26], 5-thio- $\alpha$ -, and 5-thio- $\beta$ -D-ribofuranosides [27], the molecular packing in thio-pyranosides is such that there is a distinct segregation between the polar and non-polar groups. Another common feature already reported for methyl 1,5-dithio- $\alpha$ - and  $\beta$ -D-ribofuranosides [24] is the fact that the hydrogen bonding network links the molecules so that they are packed in columns with the hydrophobic parts at the exterior of the columns.

**Molecular modeling.**—The potential energy surface computed for **1** as a function of the  $\Phi$  and  $\Psi$  torsion angles is given in Fig. 4; it can be seen that the conformational

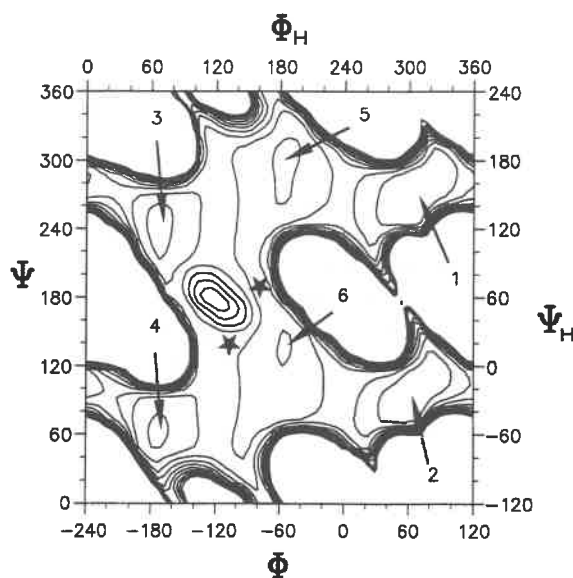


Fig. 4. Rigid potential energy surface of [4-(4-cyanobenzoyl) phenyl] 1,5-dithio- $\beta$ -D-xylopyranoside. The iso-energy contours are drawn by interpolation at 1 kcal mol<sup>-1</sup> above the minimum. The location of the six low-energy conformers is indicated on the map [→] as well as the location of the crystal structures [★].

Table 6

Summary of local minima of **1** together with their stereochemical features and their energy calculated with the Tripos force field

	$\Phi$ (°)	$\Psi$ (°)	$E_{\text{Tripos}}$ (kcal mol <sup>-1</sup> )
Crystal (1A)	-85	-177	—
Crystal (1B)	-102	144	—
C-1	65	270	-1.58
C-2	60	90	-1.00
C-3	-175	240	-0.84
C-4	-175	60	-0.77
C-5	-60	300	-0.69
C-6	-60	135	-0.61

space accessible to this molecule is very large. Another interesting feature of this map is the quasi-symmetry induced by the aromatic rings around the  $\Psi$  torsion angle. Six low-energy conformations are identified (C-1–C-6); these are listed in Table 6 in order of increasing relative energy, along with their stereochemical features.

The six energy minima fall into three classes, each member of these classes being centered around the same values of  $\Phi$ : the first (C-1–C-2) around 60° contains the global minimum, the second (C-3–C-4) is characterized by a  $\Phi$  value close to -175°, and the last (C-5–C-6) by a  $\Phi$  torsion angle of -60°. These regions are separated of the global minimum by less than 1 kcal mol<sup>-1</sup>. These data reflect the highly flexible character of this compound and all of these conformations are *prima facie* likely to occur in solution. The conformations observed in the solid state are reported on the map. The agreement between the crystallographic data and the molecular modeling results is good since the two conformers observed in the solid state are, respectively, separated by 1 and 2 kcal mol<sup>-1</sup> of the global minimum. Such discrepancy is not surprising owing to the importance of environmental effects on the stabilization of conformations in the crystal structure.

**NMR data.**—<sup>1</sup>H chemical shifts of **1** have been assigned and the through-bond (scalar) coupling networks were traced by the <sup>1</sup>H–<sup>1</sup>H COSY procedure. <sup>1</sup>H chemical shifts are given in Table 7. Experimental <sup>3</sup>J<sub>H–H</sub> values are reported in Table 8 along with the corresponding data which have been calculated for the <sup>4</sup>C<sub>1</sub> conformation of the xylopyranosyl ring according to Haasnoot et al. [28]. The mean deviation of about 10% between the two sets of parameters implies the classic <sup>4</sup>C<sub>1</sub> form for the ring of **1**. The NMR data of the aromatic protons are not included in this work since we will focus on

Table 7

<sup>1</sup>H chemical shifts (ppm) of the 1,5-dithio-β-D-xylopyranoside fragment of **1** obtained from spectral analysis and relative assignments

H-1	H-2	H-3	H-4	H-51	H-52
4.44	3.33	3.09	3.46	2.51	2.68

Table 8

Observed and calculated  $^3J_{H-H}$  coupling constants of [4-(4-cyanobenzoyl) phenyl] 1,5-dithio- $\beta$ -D-xylopyranoside **1**

Proton	$J_{Exp}$	$J_{Calc}$
$J_{1,2}$	10.5	11.0
$J_{2,3}$	8.5	9.5
$J_{3,4}$	8.5	9.4
$J_{4,51}$	4.5	3.8
$J_{4,52}$	11.0	11.7
$J_{7,8}$	8.7	
$J_{10,11}$	8.7	
$J_{14,15}$	8.5	
$J_{17,18}$	8.5	

the conformational properties of **1**. Among the 11 proton pairs which yielded a cross-peak on the phase sensitive NOESY spectrum of **1**, one corresponds to inter-residue interactions. The H-1/H-7 (H-11) pairs give a strong NOE effect. The comparison between observed and ensemble averaged values has been evaluated for the relaxation matrix (Table 9). Comparison of relaxation matrix (or NOESY intensities) is preferred to comparison of calculated and estimated proton distances [29]. When taking into account all matrix elements with observed values greater than 2% (i.e. stemming from measurable NOESY volumes), the mean deviation is 11%. Despite the weak NOESY volumes obtained for **1** owing to its  $\tau_c$  and the resulting difficulties of evaluation of cross-peak intensities, the agreement between observed and calculated data is good, as shown by the perfect agreement reached for the interaction between H-1/H-7 (H-11).

Table 9

Relaxation matrix elements observed <sup>a</sup> (*italic*) and calculated for [4-(4-cyanobenzoyl) phenyl] 1,5-dithio- $\beta$ -D-xylopyranoside **1**: the calculated values were obtained by averaging over the whole of the potential energy surface

Protons	H-1	H-2	H-3	H-4	H-51	H-52	H-7, H-11
H-1	–	0.041 (0.025)	0.022 (0.069)	0.005 (0.005)	0.050 (0.074)	0.006 (0.006)	0.036 (0.036)
H-2		–	0.068 (0.027)	0.024 (0.068)	0.010 (0.005)	0.009 (0.004)	0.011 (0.022)
H-3			–	0.027 (0.015)	0.080 (0.053)	0.008 (0.007)	0.001 (0.001)
H-4				–	0.026 (0.009)	0.094 (0.034)	0.001 (0.000)
H-51					–	0.660 (0.300)	0.002 (0.001)
H-52						–	0.001 (0.000)
H-7, H-11							–

#### 4. Conclusion

The present work characterizes, through the combined use of X-ray diffraction, molecular modeling, and NMR studies, the conformational features of a new oral venous antithrombotic agent: [4-(4-cyanobenzoyl) phenyl] 1,5-dithio- $\beta$ -D-xylopyranoside (naroparcil). The agreement reached between observed and calculated data is a satisfactory test of the validity of the conformational energy surface which may be used to safely model some of the structural features of this compound. Clearly, the studied compound is best described as a flexible molecule. The main sources of flexibility occur at the glycosidic linkage; two different conformers are observed in the crystalline state, and the experimental NMR observable can only be explained on the basis of a population of conformers belonging to a fairly broad low energy area. Consequently, no conclusion can be reached from the present study about the bio-active conformation of this antithrombotic molecule. Nevertheless, the present data provide the necessary basis for investigating the molecular features involved in the expression of biological activity, through a thorough quantitative structure activity relationship study accounting for conformational flexibility.

On the structural side, the present data have illustrated the lack of stabilizing influence arising from the exo-anomeric effect when such a C–S–C–S–C sequence is involved. They also show the necessary compensation that must occur at the three-dimensional level to accommodate both the hydrophobic and hydrophilic moieties of such a complex molecule. The neighboring molecules are first arranged so as to stack in columns to maximize their hydrophilic interactions through intermolecular hydrogen bonding.

#### Acknowledgements

The authors are very much indebted to Dr. S. Samreth, Laboratoire Fournier, Dijon, France, for providing samples of [4-(4-cyanobenzoyl) phenyl] 1,5-dithio- $\beta$ -D-xylopyranoside and for financial support to one of us (JYLQ). Appreciation is extended to Dr. B. Bachet from Laboratoire de Minéralogie Cristallographie, Université Pierre et Marie Curie, Paris for the data collection.

#### References

- [1] F. Bellamy, D. Horton, J. Millet, F. Picard, S. Samreth, and J.B. Chazan, *J. Med. Chem.*, 36 (1993) 898–903.
- [2] S. Samreth, V. Barberousse, F. Bellamy, D. Horton, P. Masson, J. Millet, P. Renaut, C. Sepulchre, and J. Theveniaux, *Actual Chim. Thérap.*, 21 (1994) 23–33.
- [3] J.-Y. Le Questel, N. Mouhous-Riou, and S. Pérez, *Carbohydr. Res.*, 265 (1994) 291–298.
- [4] J.-Y. Le Questel, N. Mouhous-Riou, and S. Pérez, *Carbohydr. Res.*, 268 (1995) 127–133.
- [5] IUPAC–IUB Commission on Biochemical Nomenclature, *Arch. Biochem. Biophys.*, 145 (1971) 405–421.
- [6] *International Tables for X-ray Crystallography*, Vol. IV, Kynoch Press, UK, 1974, pp 282–288.

- [7] G.M. Sheldrick, *SHELX76, Program for Crystal Structure Determination*, University of Cambridge, Cambridge, UK, 1976.
- [8] G.M. Sheldrick, *SHELXS86, Program for the Solution of Crystal Structures*, University of Göttingen, Germany, 1986.
- [9] S. Cros, C. Hervé du Penhoat, N. Bouchemal, H. Ohassan, A. Imberty, and S. Pérez, *Int. J. Biol. Macromol.*, 14 (1992) 313–320.
- [10] D. Neuhaus and M. Williamson, in *The Nuclear Overhauser Effect in Structural and Conformational Analysis*, VCH Publishers, 1989, p 292.
- [11] E.T. Olejniczak, R.T. Gampe, and S.W. Fesik, *J. Magn. Reson.*, 67 (1986) 28–41.
- [12] SYBYL V6.0, Tripos Associates, 1699 S. Hanley Road, Suite 303, St. Louis, MO 63144, USA.
- [13] M. Clark, R.D. III Cramer, and N. van Opdenbosh, *J. Comp. Chem.*, 10 (1989) 982–1012.
- [14] S. Pérez, C. Meyer, and A. Imberty, in A. Pullman et al. (Eds.), *Modelling of Biomolecular Structures and Mechanisms*, 1995, pp 425–454.
- [15] J.-Y. Le Questel, A. Imberty, and S. Pérez (unpublished results).
- [16] W.H. Press, B.P. Flannery, S.A. Teukolsky, and W.T. Vetterling, in *Numeric Recipes, the Art of Scientific Computing*, Cambridge University Press, Cambridge, 1986.
- [17] A.L. Spek, *Acta Crystallogr., Sect. A*, 46 (1990) C34.
- [18] G.A. Jeffrey and J.R. Ruble, and B. Sepehrnia, *Carbohydr. Res.*, 144 (1985) 197–203.
- [19] P.M. Matias and G.A. Jeffrey, *Carbohydr. Res.*, 153 (1986) 217–226.
- [20] A. Atkinson, J.R. Ruble, and G.A. Jeffrey, *Acta Crystallogr., Sect. B*, 37 (1981) 1465–1467.
- [21] R.L. Girling and G.A. Jeffrey, *Acta Crystallogr., Sect. B*, 30 (1974) 327–333.
- [22] I. Tvaroska and T. Bleha, *Adv. Carbohydr. Chem. Biochem.*, 47 (1989) 45–123.
- [23] G.A. Jeffrey, *Acta Crystallogr., Sect. B*, 46 (1990) 89–103.
- [24] E. Miler-Srenger, C. Stora, and N.A. Hughes, *Acta Crystallogr., Sect. B*, 37 (1981) 356–360.
- [25] P. Swaminathan, *Acta Crystallogr., Sect. B*, 38 (1982) 184–188.
- [26] R.L. Girling and G.A. Jeffrey, *Acta Crystallogr., Sect. B*, 29 (1973) 1006–1011.
- [27] R.L. Girling and G.A. Jeffrey, *Acta Crystallogr., Sect. B*, 29 (1973) 1102–1110.
- [28] C.A.G. Haasnoot, F.A.A.M. De Leeuw, and C. Altona, *Tetrahedron*, 36 (1980) 2783–2791.
- [29] J. Carver, *Current Opinion Struct. Biol.*, 1 (1991) 716–720.



